accurately located at the reciprocal-lattice nodes. Diffuse diffraction phenomena are mostly neglected. This extrapolation to the existence of an ideal crystal is generally out of the question even if samples of very poor quality (high mosaicity, microdomain structure, defects, ...) are investigated.

The same practice is convenient for the determination of real aperiodic structures once the type of idealized aperiodic ordering is 'known'. Again, the global ordering principle is taken as a hard constraint. For instance, the question of whether a structure is commensurately or incommensurately modulated can only be answered within a given experimental resolution. Experimentally, the ratio of the wavelength of a modulation to the period of the underlying lattice can always be determined as a rational number only. Saying that a structure is incommensurately modulated, with the above ratio being an irrational number, simply means that the experimental results can be better understood, modelled and interpreted assuming an incommensurate modulation. For example, an incommensurate charge-density wave can be moved through an ideal crystal without changing the energy of the crystal. This is not so for a commensurate modulation. In some cases, the modulation period changes with temperature in discrete steps ('devil's staircase'), generating a series of commensurate superstructures ('lock-in structures'); in other cases, a continuous variation can be observed within the experimental resolution. The latter case will be described best by an incommensurately modulated structure.

However, if only the local structure of an aperiodic crystal is of interest, a structure analysis does not take much more experimental effort than for a regular crystal. In contrast, for the analysis of the global structure, *i.e.* the characterization of the type of its 'aperiodicity', diffraction experiments with the highest possible resolution are essential. Some problems connected with the structure analysis of aperiodic crystals are dealt with in Section 4.6.4.

To determine the long-range order – whether a real 'quasicrystal' is perfectly quasiperiodic, on average quasiperiodic, a crystalline approximant or a nanodomain structure – requires information from experiments that are sensitive to changes of the global structure. Hence, one needs diffraction experiments that allow the accurate determination of the spatial intensity distribution. Consequently, the limiting factors for such experiments are the maximum spatial and intensity resolution of the diffraction and detection equipment, as well as the size and quality of the sample. Nevertheless, the resolution available on state-of-the-art standard synchrotron-beamline equipment is sufficient to test whether the ordering of atoms in an aperiodic crystal reaches the same degree of perfection as found in high-quality silicon. Of course, the higher the sample quality the more necessary it is to account for dynamical diffraction effects such as reflection broadening and displacement. Otherwise, a misinterpretation may bias the global structure modelling.

The following sections present an aid to the characterization of aperiodic crystals based on information from diffraction experiments and give a survey of aperiodic crystals from the viewpoint of the experimentally accessible reciprocal space. Characteristic features of the diffraction patterns of the different types of aperiodic crystals are shown. A standard way of determining the metrics and finding the optimum nD embedding is described. Structure-factor formulae for general and special cases are given.

4.6.2. The n-dimensional description of aperiodic crystals

4.6.2.1. Basic concepts

An incommensurate modulation of a lattice-periodic structure destroys its translational symmetry in direct and reciprocal space. In the early seventies, a method was suggested by de Wolff (1974) for restoring the lost lattice symmetry by considering the diffraction pattern of an *incommensurately modulated structure* (IMS) as a projection of an nD reciprocal lattice upon the physical space. n, the dimension of the superspace, is always larger than or equal to d, the dimension of the physical space. This leads to a simple method for the description and characterization of IMSs as well as a variety of new possibilities in their structure analysis. The nD *embedding method* is well established today and can be applied to all aperiodic crystals with reciprocal-space structure equivalent to a $\mathbb{Z}$ module with finite rank n (Janssen, 1988). The dimension of the embedding space is determined by the rank of the $\mathbb{Z}$ module, *i.e.* by the number of reciprocal-basis vectors necessary to allow for indexing all Bragg reflections with integer numbers. The point symmetry of the 3D reciprocal space (Fourier spectrum) constrains the point symmetry of the nD reciprocal lattice and restricts the number of possible nD symmetry groups.

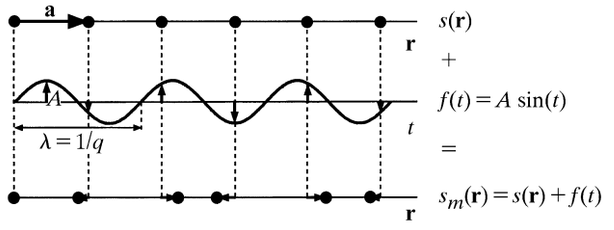

Fig. 4.6.2.1. The combination of a basic structure $s(\mathbf{r})$, with period a, and a sinusoidal modulation function $f(t)$, with amplitude A, period λ and $t = \mathbf{q} \cdot \mathbf{r}$, gives a modulated structure (MS) $s_m(\mathbf{r})$. The MS is aperiodic if a and λ are on incommensurate length scales. The filled circles represent atoms.

In the following sections, the nD descriptions of the four main classes of aperiodic crystals are demonstrated on simple 1D examples of incommensurately modulated phases, composite crystals, quasicrystals and structures with fractally shaped atomic surfaces. The main emphasis is placed on quasicrystals that show scaling symmetry, a new and unusual property in structural crystallography. A detailed discussion of the different types of 3D aperiodic crystals follows in Section 4.6.3.

4.6.2.2. 1D incommensurately modulated structures

A periodic deviation of atomic parameters from a reference structure (*basic structure*, BS) is called a *modulated structure* (MS). In the case of mutual incommensurability of the basic structure and the modulation period, the structure is called incommensurately modulated. Otherwise, it is called commensurately modulated. The modulated atomic parameters may be one or several of the following:

(a) coordinates,
(b) occupancy factors,
(c) thermal displacement parameters,
(d) orientation of the magnetic moment.

An incommensurately modulated structure can be described in a dual way by its *basic structure* $s(\mathbf{r})$ and a *modulation function* $f(t)$. This allows the structure-factor formula to be calculated and a full symmetry characterization employing representation theory to be performed (de Wolff, 1984). A more general method is the nD description: it relates the dD aperiodic incommensurately modulated structure to a periodic structure in nD space. This simplifies the symmetry analysis and structure-factor calculation, and allows more powerful structure-determination techniques.

The nD embedding method is demonstrated in the following 1D example of a displacively modulated structure. A basic structure $s(\mathbf{r}) = s(\mathbf{r} + n\mathbf{a})$, with period a and $n \in \mathbb{Z}$, is modulated by a function $f(t) = f(\mathbf{q} \cdot \mathbf{r}) = f(\alpha r) = f[\alpha r + (n a/\alpha)]$, with the satellite vector $\mathbf{q} = \alpha \mathbf{a}^*$, period $\lambda = 1/q = a/\alpha$, and α a rational or irrational number yielding a commensurately or incommensurately modulated structure $s_m(\mathbf{r})$ (Fig. 4.6.2.1).

If the 1D IMS and its 1D modulation function are properly combined in a 2D parameter space $\mathbf{V} = (\mathbf{V}^{\parallel}, \mathbf{V}^{\perp})$, a 2D lattice-

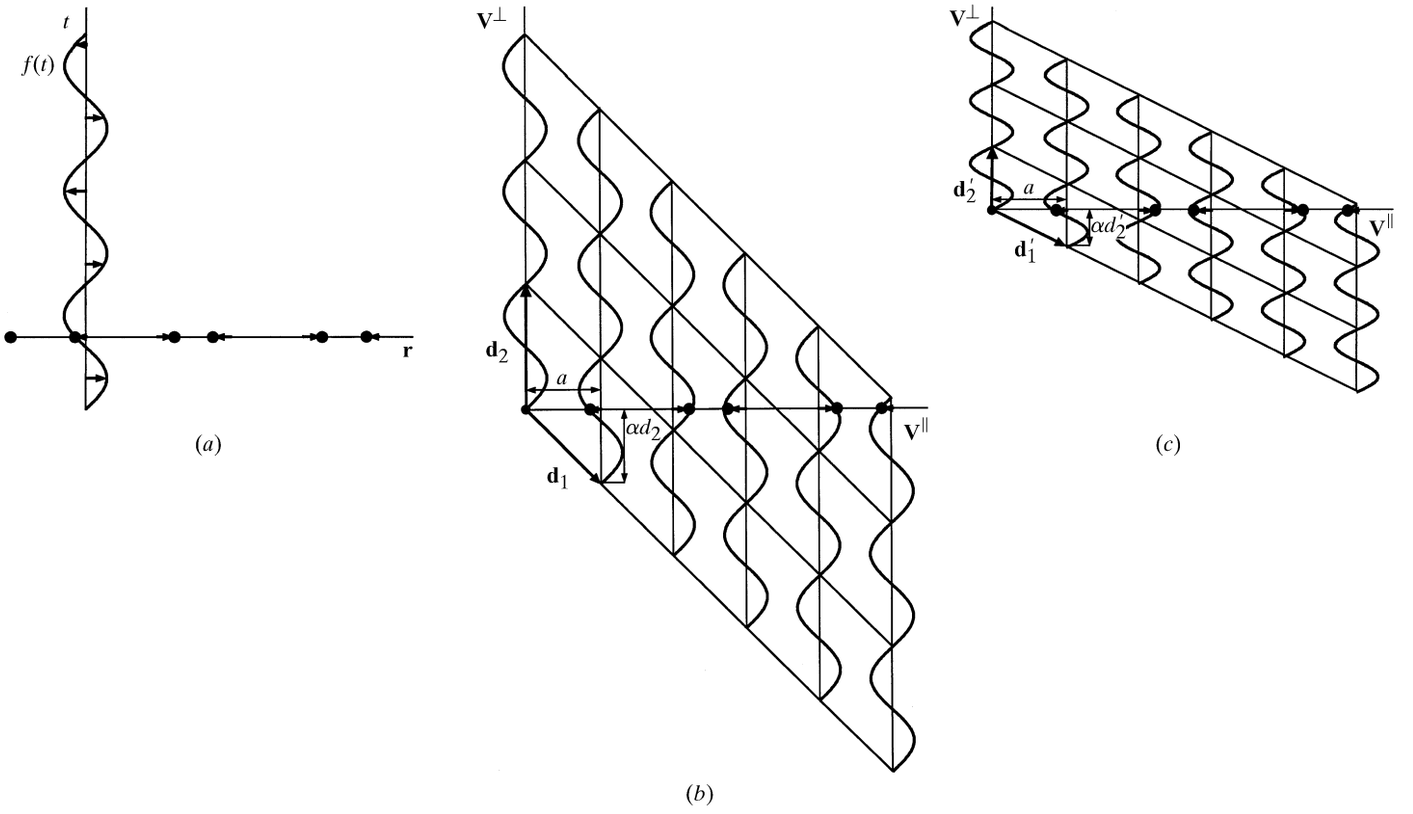

Fig. 4.6.2.2. 2D embedding of the sinusoidally modulated structure illustrated in Fig. 4.6.2.1. The correspondence between the actual displacement of an atom in the 1D structure and the modulation function defined in one additional dimension is illustrated in part (*a*). Adding to each atom its modulation function in this orthogonal dimension (perpendicular space $\mathbf{V}^{\perp}$) yields a periodic arrangement in 2D space $\mathbf{V}$, part (*b*). The MS results as a special section of the 2D periodic structure along the parallel space $\mathbf{V}^{\parallel}$. It is obvious from a comparison of (*b*) and (*c*) that the actual MS is independent of the perpendicular-space scale.

periodic structure results (Fig. 4.6.2.2). The actual atoms are generated by the intersection of the 1D physical (external, parallel) space $\mathbf{V}^{\parallel}$ with the continuous *hyperatoms*. The hyperatoms have the shape of the modulation function along the perpendicular (internal, complementary) space $\mathbf{V}^{\perp}$. They result from a convolution of the physical-space atoms with their modulation functions.

A basis $\mathbf{d}_1, \mathbf{d}_2$ (D basis) of the 2D hyperlattice $\Sigma = \{\mathbf{r} = \sum_{i=1}^{2} n_i \mathbf{d}_i | n_i \in \mathbb{Z}\}$ is given by

$$\mathbf{d}_1 = \begin{pmatrix} a \\ -\alpha/c \end{pmatrix}_V, \mathbf{d}_2 = \begin{pmatrix} 0 \\ 1/c \end{pmatrix}_V,$$

where a is the translation period of the BS and c is an arbitrary constant. The components of the basis vectors are given on a 2D orthogonal coordinate system (V basis). The components of the basis vector $\mathbf{d}_1$ are simply the parallel-space period a of the BS and α times the perpendicular-space component of the basis vector $\mathbf{d}_2$. The vector $\mathbf{d}_2$ is always parallel to the perpendicular space and its length is one period of the modulation function in arbitrary units (this is expressed by the arbitrary factor $1/c$). An atom at position $\mathbf{r}$ of the BS is displaced by an amount given by the modulation function $f(t)$, with $f(t) = f(\mathbf{q} \cdot \mathbf{r})$. Hence, the perpendicular-space variable t has to adopt the value $\mathbf{q} \cdot \mathbf{r} = \alpha \mathbf{a}^* \cdot r\mathbf{a} = \alpha r$ for the physical-space variable $\mathbf{r}$. This can be achieved by assigning the slope α to the basis vector $\mathbf{d}_1$. The choice of the parameter c has no influence on the actual MS, *i.e.* the way in which the 2D structure is cut by the parallel space (Fig. 4.6.2.2*c*).

The basis of the lattice $\Sigma^* = \{\mathbf{H} = \sum_{i=1}^{2} h_i \mathbf{d}_i^* | h_i \in \mathbb{Z}\}$, reciprocal to Σ, can be obtained from the condition $\mathbf{d}_i \cdot \mathbf{d}_j^* = \delta_{ij}$:

$$\mathbf{d}_1^* = \begin{pmatrix} a^* \\ 0 \end{pmatrix}_V, \mathbf{d}_2^* = \begin{pmatrix} \alpha a^* \\ c \end{pmatrix}_V,$$

with $a^* = 1/a$. The metric tensors for the reciprocal and direct 2D lattices for $c = 1$ are

$$G^* = \begin{pmatrix} a^{*2} & \alpha a^{*2} \\ \alpha a^{*2} & 1 + \alpha^2 a^{*2} \end{pmatrix} \quad \text{and} \quad G = \begin{pmatrix} a^2 + \alpha^2 & -\alpha \\ -\alpha & 1 \end{pmatrix}.$$

The choice of an arbitrary number for c has no influence on the metrics of the physical-space components of the IMS in direct or reciprocal space.

The Fourier transform of the *hypercrystal* depicted in Fig. 4.6.2.2 gives the weighted reciprocal lattice shown in Fig. 4.6.2.3. The 1D diffraction pattern $M^* = \{\mathbf{H}^{\parallel} = \sum_{i=1}^{2} h_i \mathbf{a}_i^* | h_i \in \mathbb{Z}\}$ in physical space is obtained by a projection of the weighted 2D reciprocal lattice Σ^* along $\mathbf{V}^{\perp}$ as the Fourier transform of a section in direct space corresponds to a projection in reciprocal space and *vice versa*:

$$M^* = \{\mathbf{H}^{\parallel}\} \xleftarrow{\text{projection } \pi^{\parallel} \text{ onto } \mathbf{V}^{\parallel}} \Sigma^* = \{\mathbf{H} = (\mathbf{H}^{\parallel}, \mathbf{H}^{\perp})\}.$$

Reciprocal-lattice points lying in physical space are referred to as *main reflections*, all others as *satellite reflections*. All Bragg reflections can be indexed with integer numbers h_1, h_2 in the 2D description $\mathbf{H} = h_1 \mathbf{d}_1^* + h_2 \mathbf{d}_2^*$. In the physical-space description, the diffraction vector can be written as $\mathbf{H}^{\parallel} = h\mathbf{a}^* + m\mathbf{q} = \mathbf{a}^*(h_1 + \alpha h_2)$, with $\mathbf{q} = \alpha \mathbf{a}^*$ for the satellite vector and $m \in \mathbb{Z}$ the order of the satellite reflection. For a detailed discussion of the

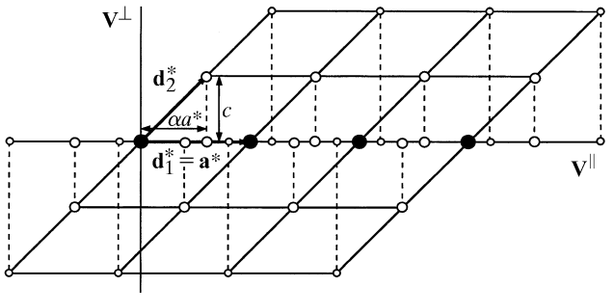

Fig. 4.6.2.3. Schematic representation of the 2D reciprocal-space embedding of the 1D sinusoidally modulated structure depicted in Figs. 4.6.2.1 and 4.6.2.2. Main reflections are marked by filled circles and satellite reflections by open circles. The sizes of the circles are roughly related to the reflection intensities. The actual 1D diffraction pattern of the 1D MS results from a projection of the 2D reciprocal space onto the parallel space. The correspondence between 2D reciprocal-lattice positions and their projected images is indicated by dashed lines.

embedding and symmetry description of IMSs see, for example, Janssen *et al.* (2004).

A commensurately modulated structure with $\alpha' = m/n$ and $\lambda = (n/m)a$, $m, n \in \mathbb{Z}$, and with $c = 1$, can be generated by shearing the 2D lattice Σ with a shear matrix S_m:

$$\mathbf{d}_i' = \sum_{j=1}^{2} S_{mij}\mathbf{d}_j, \text{ with } S_m = \begin{pmatrix} 1 & -x \\ 0 & 1 \end{pmatrix}_D \text{ and } x = \alpha' - \alpha,$$

$$\mathbf{d}_1' = \mathbf{d}_1 - x\mathbf{d}_2 = \begin{pmatrix} a \\ -\alpha \end{pmatrix}_V - (\alpha' - \alpha)\begin{pmatrix} 0 \\ 1 \end{pmatrix}_V = \begin{pmatrix} a \\ -\alpha' \end{pmatrix}_V,$$

$$\mathbf{d}_2' = \mathbf{d}_2 = \begin{pmatrix} 0 \\ 1 \end{pmatrix}_V.$$

The subscript D (V) following the shear matrix indicates that it is acting on the D (V) basis. The shear matrix does not change the distances between the atoms in the basic structure. In reciprocal space, using the inverted and transposed shear matrix, one obtains

$$\mathbf{d}_i^{*\prime} = \sum_{j=1}^{2} (S_m^{-1})_{ij}^T \mathbf{d}_j^*, \text{ with } (S_m^{-1})^T = \begin{pmatrix} 1 & 0 \\ x & 1 \end{pmatrix}_D \text{ and } x = \alpha' - \alpha,$$

$$\mathbf{d}_1^{*\prime} = \mathbf{d}_1^* = \begin{pmatrix} a^* \\ 0 \end{pmatrix}_V,$$

$$\mathbf{d}_2^{*\prime} = x\mathbf{d}_1^* + \mathbf{d}_2^* = (\alpha' - \alpha)\begin{pmatrix} a^* \\ 0 \end{pmatrix}_V + \begin{pmatrix} \alpha a^* \\ 1 \end{pmatrix}_V = \begin{pmatrix} \alpha' a^* \\ 1 \end{pmatrix}_V.$$

4.6.2.3. 1D composite structures

In the simplest case, a *composite structure* (CS) consists of two intergrown periodic structures with mutually incommensurate lattices. Owing to mutual interactions, each subsystem may be modulated with the period of the other. Consequently, CSs can be considered as coherent intergrowths of two or more incommensurately modulated substructures. The substructures have at least the origin of their reciprocal lattices in common. However, in all known cases, at least one common reciprocal-lattice plane exists. This means that at least one particular projection of the composite structure exhibits full lattice periodicity.

The unmodulated (basic) 1D subsystems of a 1D incommensurate intergrowth structure can be related to each other in a 2D parameter space $\mathbf{V} = (\mathbf{V}^{\parallel}, \mathbf{V}^{\perp})$ (Fig. 4.6.2.4). The actual atoms result from the intersection of the physical space $\mathbf{V}^{\parallel}$ with the hypercrystal. The hyperatoms correspond to a convolution of the

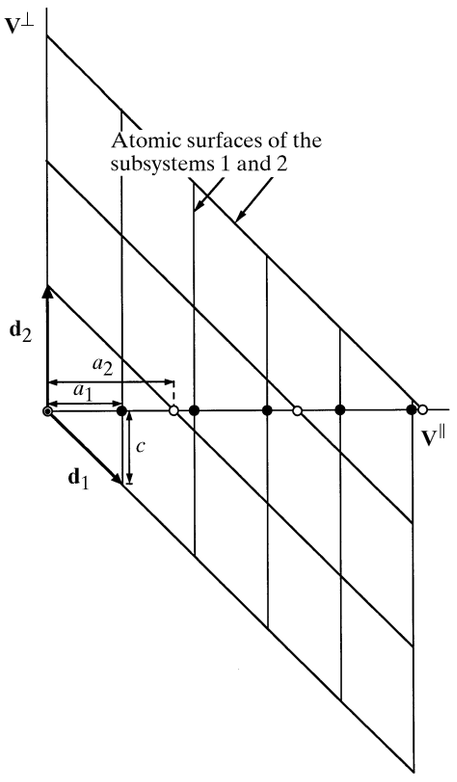

Fig. 4.6.2.4. 2D embedding of a 1D composite structure without mutual interaction of the subsystems. Filled and empty circles represent the atoms of the unmodulated substructures with periods a_1 and a_2, respectively. The atoms result from the parallel-space cut of the linear atomic surfaces parallel to $\mathbf{d}_1$ and $\mathbf{d}_2$.

real atoms with infinite lines parallel to the basis vectors $\mathbf{d}_1$ and $\mathbf{d}_2$ of the 2D hyperlattice $\Sigma = \{\mathbf{r} = \sum_{i=1}^{2} n_i\mathbf{d}_i | n_i \in \mathbb{Z}\}$.

An appropriate basis is given by

$$\mathbf{d}_1 = \begin{pmatrix} a_1 \\ -c \end{pmatrix}_V, \mathbf{d}_2 = \begin{pmatrix} 0 \\ c(a_2/a_1) \end{pmatrix}_V,$$

where a_1 and a_2 are the lattice parameters of the two substructures and c is an arbitrary constant. Taking into account the interactions between the subsystems, each one becomes modulated with the period of the other. Consequently, in the 2D description, the shape of the hyperatoms is determined by their modulation functions (Fig. 4.6.2.5).

A basis of the reciprocal lattice $\Sigma^* = \{\mathbf{H} = \sum_{i=1}^{2} h_i\mathbf{d}_i^* | h_i \in \mathbb{Z}\}$ can be obtained from the condition $\mathbf{d}_i \cdot \mathbf{d}_j^* = \delta_{ij}$:

$$\mathbf{d}_1^* = \begin{pmatrix} a_1^* \\ 0 \end{pmatrix}_V, \mathbf{d}_2^* = \begin{pmatrix} a_2^* \\ (a_2^*/ca_1^*) \end{pmatrix}_V.$$

The metric tensors for the reciprocal and the direct 2D lattices for $c = 1$ are

$$G^* = \begin{pmatrix} a_1^{*2} & a_1^* a_2^* \\ a_1^* a_2^* & (1 + a_1^{*2})(a_2^*/a_1^*)^2 \end{pmatrix} \text{ and } G = \begin{pmatrix} 1 + a_1^2 & -a_2/a_1 \\ -a_2/a_1 & (a_2/a_1)^2 \end{pmatrix}.$$

The Fourier transforms of the hypercrystals depicted in Figs. 4.6.2.4 and 4.6.2.5 correspond to the weighted reciprocal lattices illustrated in Figs. 4.6.2.6 and 4.6.2.7. The 1D diffraction patterns $M^* = \{\mathbf{H}^{\parallel} = \sum_{i=1}^{2} h_i\mathbf{a}_i^* | h_i \in \mathbb{Z}\}$ in physical space are obtained by a projection of the weighted 2D reciprocal lattices Σ^* upon $\mathbf{V}^{\parallel}$. All Bragg reflections can be indexed with integer numbers h_1, h_2

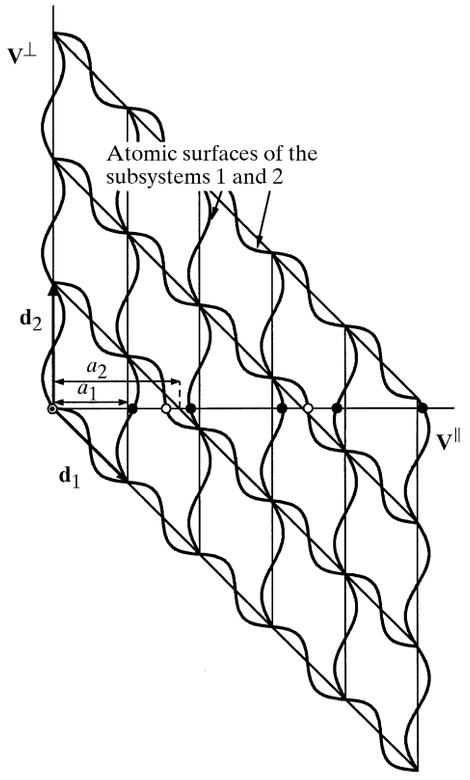

Fig. 4.6.2.5. 2D embedding of a 1D composite structure with mutual interaction of the subsystems causing modulations. Filled and empty circles represent the modulated substructures with periods a_1 and a_2 of the basic substructures, respectively. The atoms result from the parallel-space cut of the sinusoidal atomic surfaces running parallel to $\mathbf{d}_1$ and $\mathbf{d}_2$.

in both the 2D description $\mathbf{H} = h_1\mathbf{d}_1^* + h_2\mathbf{d}_2^*$ and in the 1D physical-space description with two parallel basis vectors $\mathbf{H}^{\parallel} = h_1\mathbf{a}_1^* + h_2\mathbf{a}_2^*$.

The reciprocal-lattice points $\mathbf{H} = h_1\mathbf{d}_1^*$ and $\mathbf{H} = h_2\mathbf{d}_2^*$, h_1, $h_2 \in \mathbb{Z}$, on the main axes $\mathbf{d}_1^*$ and $\mathbf{d}_2^*$ are the main reflections of the two substructures. All other reflections are referred to as satellite reflections. Their intensities differ from zero only in the case of modulated substructures. Each reflection of one subsystem coincides with exactly one reflection of the other subsystem.

4.6.2.4. 1D quasiperiodic structures

The Fibonacci sequence, the best investigated example of a 1D quasiperiodic structure, can be obtained from the substitution rule σ: S $\rightarrow$ L, L $\rightarrow$ LS, replacing the letter S by L and the letter L by the word LS (see *e.g.* Luck *et al.*, 1993). Applying the substitution matrix

$$S = \begin{pmatrix} 0 & 1 \\ 1 & 1 \end{pmatrix}$$

associated with σ, this rule can be written in the form

$$\begin{pmatrix} \mathrm{S} \\ \mathrm{L} \end{pmatrix} \rightarrow \begin{pmatrix} 0 & 1 \\ 1 & 1 \end{pmatrix}\begin{pmatrix} \mathrm{S} \\ \mathrm{L} \end{pmatrix} = \begin{pmatrix} \mathrm{L} \\ \mathrm{L}+\mathrm{S} \end{pmatrix}.$$

S gives the sum of letters, L + S = S + L, and not their order. Consequently, the same substitution matrix can also be applied, for instance, to the substitution σ': S $\rightarrow$ L, L $\rightarrow$ SL. The repeated action of S on the alphabet $A = \{\mathrm{S}, \mathrm{L}\}$ yields the words $A_n = \sigma^n(\mathrm{S})$ and $B_n = \sigma^n(\mathrm{L}) = A_{n+1}$ as illustrated in Table 4.6.2.1. The frequencies of letters contained in the words A_n and B_n can

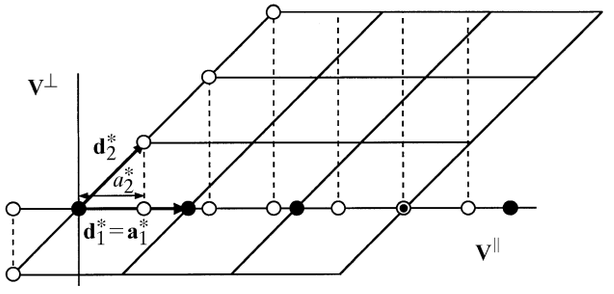

Fig. 4.6.2.6. Schematic representation of the reciprocal space of the embedded 1D composite structure depicted in Fig. 4.6.2.4. Filled and empty circles represent the reflections generated by the substructures with periods a_1 and a_2, respectively. The actual 1D diffraction pattern of the 1D CS results from a projection of the 2D reciprocal space onto the parallel space. The correspondence between 2D reciprocal-lattice positions and their projected images is indicated by dashed lines.

be calculated by applying the nth power of the transposed substitution matrix on the unit vector. From

$$\begin{pmatrix} \nu_{n+1}^A \\ \nu_{n+1}^B \end{pmatrix} = S^T \begin{pmatrix} \nu_n^A \\ \nu_n^B \end{pmatrix}$$

it follows that

$$\begin{pmatrix} \nu_n^A \\ \nu_n^B \end{pmatrix} = (S^T)^n \begin{pmatrix} 1 \\ 1 \end{pmatrix}.$$

In the case of the Fibonacci sequence, ν_n^B gives the total number of letters S and L, and ν_n^A the number of letters L.

An infinite Fibonacci sequence, *i.e.* a word B_n with $n \rightarrow \infty$, remains invariant under inflation (deflation). Inflation (deflation) means that the number of letters L, S increases (decreases) under the action of the (inverted) substitution matrix S. Inflation and deflation represent self-similarity (scaling) symmetry operations on the infinite Fibonacci sequence. A more detailed discussion of the scaling properties of the Fibonacci chain in direct and reciprocal space will be given later.

The Fibonacci numbers $F_n = F_{n-1} + F_{n-2}$ form a series with $\lim_{n\rightarrow\infty}(F_{n+1}/F_n) = \tau$ {the golden mean $\tau = [1 + (5)^{1/2}]/2 = 2\cos(\pi/5) = 1.618\ldots$}. The ratio of the frequencies of L and S

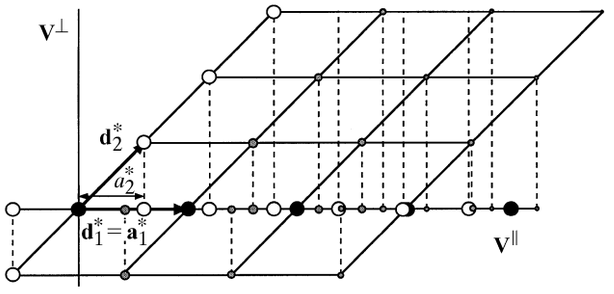

Fig. 4.6.2.7. Schematic representation of the reciprocal space of the embedded 1D composite structure depicted in Fig. 4.6.2.5. Filled and empty circles represent the main reflections of the two subsystems. The satellite reflections generated by the modulated substructures are shown as grey circles. The diameters of the circles are roughly proportional to the intensities of the reflections. The actual 1D diffraction pattern of the 1D CS results from a projection of the 2D reciprocal space onto the parallel space. The correspondence between 2D reciprocal-lattice positions and their projected images is indicated by dashed lines.

Table 4.6.2.1. *Expansion of the Fibonacci sequence* $B_n = \sigma^n(\mathrm{L})$ *by repeated action of the substitution rule* σ: $\mathrm{S} \rightarrow \mathrm{L}$, $\mathrm{L} \rightarrow \mathrm{LS}$

ν_L, ν_S are the frequencies of the letters L and S in word B_n.

B_n	ν_L	ν_S	n
L	1	0	0
LS	1	1	1
LSL	2	1	2
LSLLS	3	2	3
LSLLSLSL	5	3	4
LSLLSLSLLSLLS	8	5	5
LSLLSLSLLSLLSLSLLSLSL	13	8	6
	⋮	⋮	⋮
	F_{n+1}	F_n	n

in the Fibonacci sequence converges to τ if the sequence goes to infinity. The continued fraction expansion of the golden mean τ,

$$\tau = 1 + \cfrac{1}{1 + \cfrac{1}{1 + \cfrac{1}{1 + \ldots}}},$$

contains only the number 1. This means that τ is the 'most irrational' number, *i.e.* the irrational number with the worst truncated continued fraction approximation to it. This might be one of the reasons for the stability of quasiperiodic systems, where τ plays a role. The strong irrationality may impede the lock-in into commensurate systems (*rational approximants*).

By associating intervals (*e.g.* atomic distances) with length ratio τ to 1 to the letters L and S, a quasiperiodic structure $s(\mathbf{r})$ (*Fibonacci chain*) can be obtained. The invariance of the ratio of lengths $\mathrm{L/S} = (\mathrm{L} + \mathrm{S})/\mathrm{L} = \tau$ is responsible for the invariance of the Fibonacci chain under scaling by a factor τ^n, $n \in \mathbb{Z}$. Owing to a minimum atomic distance S in real crystal structures, the full set of inverse symmetry operators τ^{-n} does not exist. Consequently, the set of scaling operators $s = \{\tau^0 = 1, \tau^1, \ldots\}$ forms only a semi-group, *i.e.* an associative groupoid. Groupoids are the most general algebraic sets satisfying only one of the group axioms: the associative law. The scaling properties of the Fibonacci sequence can be derived from the eigenvalues of the scaling matrix S. For this purpose the equation

$$\det|S - \lambda I| = 0$$

with eigenvalue λ and unit matrix I has to be solved. The evaluation of the determinant yields the characteristic polynomial

$$\lambda^2 - \lambda - 1 = 0,$$

yielding in turn the eigenvalues $\lambda_1 = [1 + (5)^{1/2}]/2 = \tau$, $\lambda_2 = [1 - (5)^{1/2}]/2 = -1/\tau$ and the eigenvectors

$$\mathbf{w}_1 = \begin{pmatrix} 1 \\ \tau \end{pmatrix}, \quad \mathbf{w}_2 = \begin{pmatrix} 1 \\ -1/\tau \end{pmatrix}.$$

Rewriting the eigenvalue equation gives for the first (*i.e.* the largest) eigenvalue

$$\begin{pmatrix} 0 & 1 \\ 1 & 1 \end{pmatrix}\begin{pmatrix} 1 \\ \tau \end{pmatrix} = \begin{pmatrix} \tau \\ 1 + \tau \end{pmatrix} = \begin{pmatrix} \tau \\ \tau^2 \end{pmatrix} = \tau\begin{pmatrix} 1 \\ \tau \end{pmatrix}.$$

Identifying the eigenvector

$$\begin{pmatrix} 1 \\ \tau \end{pmatrix}$$

with

$$\begin{pmatrix} \mathrm{S} \\ \mathrm{L} \end{pmatrix}$$

shows that an infinite Fibonacci sequence $s(\mathbf{r})$ remains invariant under scaling by a factor τ. This scaling operation maps each new lattice vector $\tau\mathbf{r}$ upon a vector $\mathbf{r}$ of the original lattice:

$$s(\tau\mathbf{r}) = s(\mathbf{r}).$$

Considering periodic lattices, these eigenvalues are integer numbers. For quasiperiodic 'lattices' (*quasilattices*) they always correspond to *algebraic numbers* (*Pisot numbers*). A Pisot number is the solution of a polynomial equation with integer coefficients. It is larger than one, whereas the modulus of its conjugate is smaller than unity: $\lambda_1 > 1$ and $|\lambda_2| < 1$ (Luck *et al.*, 1993). The total lengths l_n^A and l_n^B of the words A_n, B_n can be determined from the equations $l_n^A = \lambda_1^n l^A$ and $l_n^B = \lambda_1^n l^B$ with the eigenvalue λ_1. The left Perron–Frobenius eigenvector $\mathbf{w}_1$ of S, *i.e.* the left eigenvector associated with λ_1, determines the ratio S:L to 1:τ. The right Perron–Frobenius eigenvector $\mathbf{w}_1$ of S associated with λ_1 gives the relative frequencies, 1 and τ, for the letters S and L (for a definition of the Perron–Frobenius theorem see Luck *et al.*, 1993, and references therein).

The general case of an alphabet $A = \{\mathrm{L}_1 \ldots \mathrm{L}_k\}$ with k letters (intervals) L_i, of which at least two are on incommensurate length scales and which transform with the substitution matrix S,

$$\mathrm{L}_i' \rightarrow \sum_{j=1}^{k} S_{ij}\mathrm{L}_j,$$

can be treated analogously. S is a $k \times k$ matrix with non-negative integer coefficients. Its eigenvalues are solutions of a polynomial equation of rank k with integer coefficients (algebraic or Pisot numbers). The dimension n of the embedding space is generically equal to the number of letters (intervals) k involved by the substitution rule. From substitution rules, infinitely many different 1D quasiperiodic sequences can be generated. However, their atomic surfaces in the nD description are generically of fractal shape (see Section 4.6.2.5).

The quasiperiodic 1D density distribution $\rho(\mathbf{r})$ of the Fibonacci chain can be represented by the Fourier series

$$\rho(\mathbf{r}) = (1/V)\sum_{\mathbf{H}^\parallel} F(\mathbf{H}^\parallel)\exp(-2\pi i\mathbf{H}^\parallel \cdot \mathbf{r}),$$

with $\mathbf{H}^\parallel \in \mathbb{R}$ (the set of real numbers). The Fourier coefficients $F(\mathbf{H}^\parallel)$ form a Fourier module $M^* = \{\mathbf{H}^\parallel = \sum_{i=1}^{2} h_i\mathbf{a}_i^* | h_i \in \mathbb{Z}\}$ equivalent to a $\mathbb{Z}$ module of rank 2. Thus a periodic function in 2D space can be defined by

$$\rho(\mathbf{r}^\parallel, \mathbf{r}^\perp) = (1/V)\sum_{\mathbf{H}} F(\mathbf{H})\exp[-2\pi i(\mathbf{H}^\parallel \cdot \mathbf{r}^\parallel + \mathbf{H}^\perp \cdot \mathbf{r}^\perp)],$$

where $\mathbf{r} = (\mathbf{r}^\parallel, \mathbf{r}^\perp) \in \Sigma$ and $\mathbf{H} = (\mathbf{H}^\parallel, \mathbf{H}^\perp) \in \Sigma^*$ are, by construction, direct- and reciprocal-lattice vectors (Figs. 4.6.2.8 and 4.6.2.9):

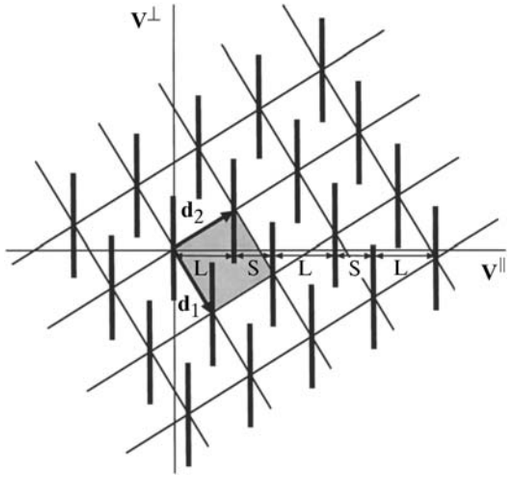

Fig. 4.6.2.8. 2D embedding of the Fibonacci chain. The short and long distances S and L, generated by the intersection of the atomic surfaces with the physical space $\mathbf{V}^\parallel$, are indicated. The atomic surfaces are represented by bars parallel to $\mathbf{V}^\perp$. Their lengths correspond to the projection of one unit cell (shaded) upon $\mathbf{V}^\perp$.

$$\mathbf{r} = n_1\mathbf{d}_1 + n_2\mathbf{d}_2, \text{ with } \mathbf{d}_1 = \frac{1}{a^*(2+\tau)}\begin{pmatrix}1\\-\tau\end{pmatrix}_V,$$

$$\mathbf{d}_2 = \frac{1}{a^*(2+\tau)}\begin{pmatrix}\tau\\1\end{pmatrix}_V;$$

$$\mathbf{H} = h_1\mathbf{d}_1^* + h_2\mathbf{d}_2^*, \text{ with } \mathbf{d}_1^* = a^*\begin{pmatrix}1\\-\tau\end{pmatrix}_V, \mathbf{d}_2^* = a^*\begin{pmatrix}\tau\\1\end{pmatrix}_V.$$

The 1D Fibonacci chain results from the cut of the parallel (physical) space with the 2D lattice Σ decorated with line elements for the *atomic surfaces* (*acceptance domains*). In this description, the atomic surfaces correspond simply to the projection of one 2D unit cell upon the perpendicular-space coordinate. This satisfies the condition that each unit cell contributes exactly to one point of the Fibonacci chain (*primitive unit cell*). The physical space $\mathbf{V}^\parallel$ is related to the eigenspace of the substitution matrix S associated with its eigenvalue $\lambda_1 = \tau$. The perpendicular space $\mathbf{V}^\perp$ corresponds to the eigenspace of the substitution matrix S associated with its eigenvalue $\lambda_2 = -1/\tau$. Thus, the physical space scales to powers of τ and the perpendicular space to powers of $-1/\tau$.

By block-diagonalization, the reducible substitution (scaling) matrix S can be decomposed into two non-equivalent irreducible representations. These can be assigned to the two 1D orthogonal subspaces $\mathbf{V}^\parallel$ and $\mathbf{V}^\perp$ forming the 2D embedding space $\mathbf{V} = \mathbf{V}^\parallel \oplus \mathbf{V}^\perp$. Thus, using $WSW^{-1} = S_V = S_V^\parallel \oplus S_V^\perp$, where

$$W = \begin{pmatrix}1 & \tau\\ -\tau & 1\end{pmatrix} = \begin{pmatrix}\mathbf{d}_1^* & \mathbf{d}_2^*\end{pmatrix},$$

one obtains

$$\begin{pmatrix}1 & \tau\\ -\tau & 1\end{pmatrix}\begin{pmatrix}0 & 1\\ 1 & 1\end{pmatrix}_D\begin{pmatrix}1 & \tau\\ -\tau & 1\end{pmatrix}^{-1} = \left(\begin{array}{c|c}\tau & 0\\ \hline 0 & -1/\tau\end{array}\right)_V = \left(\begin{array}{c|c}S^\parallel & 0\\ \hline 0 & S^\perp\end{array}\right)_V,$$

the scaling operations $S^\parallel$ and $S^\perp$ in parallel and in perpendicular space as indicated by the partition lines.

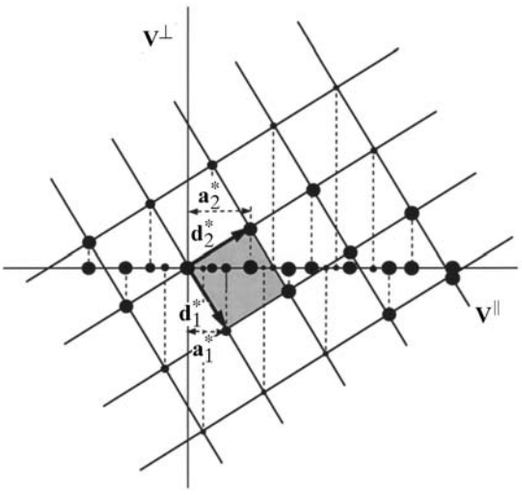

Fig. 4.6.2.9. Schematic representation of the reciprocal space of the embedded Fibonacci chain depicted in Fig. 4.6.2.8. The physical-space reciprocal basis $\mathbf{a}_1^*$ and $\mathbf{a}_2^*$ is marked. The diameters of the filled circles are roughly proportional to the reflection intensities. One 2D reciprocal-lattice unit cell is shadowed. The actual 1D diffraction pattern of the 1D Fibonacci chain results from a projection of the 2D reciprocal space onto the parallel space. The correspondence between 2D reciprocal-lattice positions and their projected images is indicated by dashed lines.

The metric tensors for the reciprocal and the direct 2D square lattices read

$$G^* = |a^*|^2(2+\tau)\begin{pmatrix}1 & 0\\ 0 & 1\end{pmatrix} \text{ and } G = \frac{1}{|a^*|^2(2+\tau)}\begin{pmatrix}1 & 0\\ 0 & 1\end{pmatrix}.$$

The short distance S of the Fibonacci sequence is related to a^* by

$$\begin{aligned} S &= 1/[a^*(2+\tau)]\\ &= \min\left\{\left|\pi^\parallel(\mathbf{d}_i - \mathbf{d}_j)\right| \,\middle|\, \left|\pi^\perp(\mathbf{d}_i - \mathbf{d}_j)\right| < \Omega_{\rm AS} \wedge i, j \in \mathbb{Z}\right\}, \end{aligned}$$

with the projectors $\pi^\parallel$ and $\pi^\perp$ onto $\mathbf{V}^\parallel$ and $\mathbf{V}^\perp$. The *point density* $\rho_{\rm p}$ of the Fibonacci chain, *i.e.* the number of vertices per unit length, can be calculated using the formula

$$\rho_{\rm p} = \frac{\Omega_{\rm AS}}{\Omega_{\rm UC}} = \frac{(1+\tau)/[a^*(2+\tau)]}{1/[|a^*|^2(2+\tau)]} = a^*\tau^2,$$

where $\Omega_{\rm AS}$ and $\Omega_{\rm UC}$ are the areas of the atomic surface and of the 2D unit cell, respectively.

For an infinite Fibonacci sequence generated from the intervals S and L an average distance d can be calculated:

$$d = \lim_{n\to\infty}\frac{F_n\mathrm{S} + F_{n+1}\mathrm{L}}{F_n + F_{n+1}} = \lim_{n\to\infty}\frac{F_n(\mathrm{S}+\tau\mathrm{L})}{F_n(1+\tau)} = \frac{\mathrm{S}(1+\tau^2)}{(1+\tau)} = (3-\tau)\mathrm{S}.$$

Therefrom, the point density can also be calculated:

$$\rho_{\rm p} = 1/d = 1/[(3-\tau)\mathrm{S}] = [a^*(2+\tau)]/(3-\tau) = a^*\tau^2.$$

An approximant structure of the Fibonacci sequence with a unit cell containing m intervals L and n intervals S can be generated by shearing the 2D lattice Σ by the shear matrix S_m,

$$S_m = \frac{1}{2+\tau}\begin{pmatrix} \tau^2 + x\tau + 1 & -x \\ x\tau^2 & \tau^2 - x\tau + 1 \end{pmatrix}_D,$$

where $x = (n\tau - m)/(m\tau + n)$:

$$\begin{aligned}
\mathbf{d}_i' &= \sum_{j=1}^{2} S_{mij}\mathbf{d}_j; \\
\mathbf{d}_1' &= \frac{1}{2+\tau}\left[(\tau^2 + x\tau + 1)\mathbf{d}_1 - x\mathbf{d}_2\right] \\
&= \frac{1}{(2+\tau)a^*}\begin{pmatrix} 1 \\ -\tau - x \end{pmatrix}_V \\
&= \frac{1}{(2+\tau)a^*}\begin{pmatrix} 1 \\ -\dfrac{2n\tau + m\tau}{m\tau + n} \end{pmatrix}_V, \\
\mathbf{d}_2' &= \frac{1}{2+\tau}\left[x\tau^2\mathbf{d}_1 + (\tau^2 - x\tau + 1)\mathbf{d}_2\right] \\
&= \frac{1}{(2+\tau)a^*}\begin{pmatrix} \tau \\ -x\tau + 1 \end{pmatrix}_V \\
&= \frac{1}{(2+\tau)a^*}\begin{pmatrix} \tau \\ \dfrac{2m\tau - n\tau}{m\tau + n} \end{pmatrix}_V.
\end{aligned}$$

This shear matrix does not change the magnitudes of the intervals L and S. In reciprocal space the inverted and transposed shear matrix is applied on the reciprocal basis,

$$(S_m^{-1})^T = \frac{1}{2+\tau}\begin{pmatrix} \tau^2 - x\tau + 1 & -x\tau^2 \\ x & \tau^2 + x\tau + 1 \end{pmatrix}_D,$$

where $x = (n\tau - m)/(m\tau + n)$:

$$\begin{aligned}
\mathbf{d}_i^{*'} &= \sum_{j=1}^{2} (S_m^{-1})_{ij}^T \mathbf{d}_j^*; \\
\mathbf{d}_1^{*'} &= \frac{1}{2+\tau}\left[(\tau^2 - x\tau + 1)\mathbf{d}_1^* - x\tau^2\mathbf{d}_2^*\right] \\
&= a^*\begin{pmatrix} 1 - x\tau \\ -\tau \end{pmatrix}_V \\
&= a^*\begin{pmatrix} \dfrac{2m\tau - n\tau}{m\tau + n} \\ -\tau \end{pmatrix}_V, \\
\mathbf{d}_2^{*'} &= \frac{1}{2+\tau}\left[x\mathbf{d}_1^* + (\tau^2 + x\tau + 1)\mathbf{d}_2^*\right] \\
&= a^*\begin{pmatrix} \tau + x \\ 1 \end{pmatrix}_V \\
&= a^*\begin{pmatrix} \dfrac{2n\tau + m\tau}{m\tau + n} \\ 1 \end{pmatrix}_V.
\end{aligned}$$

The point $x_n(t)$ of the nth interval L or S of an infinite Fibonacci sequence is given by

$$x_n(t) = \{x_0 + n(3 - \tau) - (\tau - 1)[\mathrm{frac}(n\tau + t) - (1/2)]\}\mathrm{S},$$

where t is the phase of the modulation function $y(t) = (\tau - 1)[\mathrm{frac}(n\tau + t) - (1/2)]$ (Janssen, 1986). Thus, the Fibonacci sequence can also be dealt with as an incommensurately modulated structure. This is a consequence of the fact that for 1D structures only the crystallographic point symmetries 1 and $\bar{1}$ allow the existence of a periodic average structure.

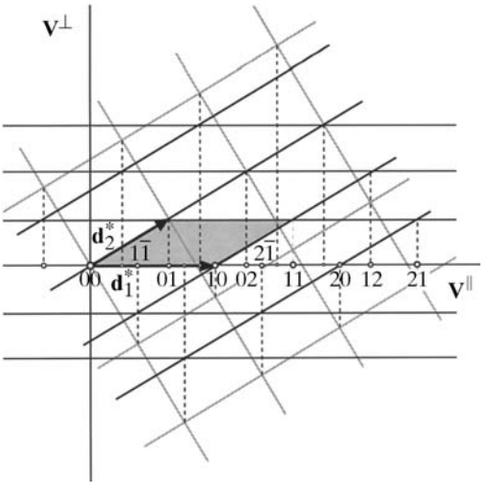

Fig. 4.6.2.10. Reciprocal space of the embedded Fibonacci chain as a modulated structure. Several main and satellite reflections are indexed. The square reciprocal lattice of the quasicrystal description illustrated in Fig. 4.6.2.9 is indicated by grey lines. The reflections located on $\mathbf{V}^\parallel$ can be considered to be projected either from the 2D square lattice of the embedding as for a QS or from the 2D oblique lattice of the embedding as for an IMS.

The embedding of the Fibonacci chain as an incommensurately modulated structure can be performed as follows:

(1) select a subset $\Lambda^* \subset M^*$ of strong reflections for main reflections $\mathbf{H} = h\mathbf{a}^*, h \in \mathbb{Z}$;

(2) define a satellite vector $\mathbf{q} = \alpha\mathbf{a}^*$ pointing from each main reflection to the next satellite reflection.

One possible way of indexing based on the same $\mathbf{a}^*$ as defined above is illustrated in Fig. 4.6.2.10. The scattering vector is given by $\mathbf{H}^\parallel = h(\tau + 1)\mathbf{a}^* + mq$, where $\mathbf{q} = \tau\mathbf{a}^*$, or, in the 2D representation, $\mathbf{H} = h_1\mathbf{d}_1^* + h_2\mathbf{d}_2^*$, where

$$\mathbf{d}_1^* = a^*\begin{pmatrix} 1 + \tau \\ 0 \end{pmatrix}_V$$

and

$$\mathbf{d}_2^* = a^*\begin{pmatrix} \tau \\ 1 \end{pmatrix}_V,$$

with the direct basis

$$\mathbf{d}_1 = \frac{1}{a^*(1+\tau)}\begin{pmatrix} 1 \\ -\tau \end{pmatrix}_V, \quad \mathbf{d}_2 = \frac{1}{a^*}\begin{pmatrix} 0 \\ 1 \end{pmatrix}_V.$$

The modulation function is saw-tooth-like (Fig. 4.6.2.11).

4.6.2.5. 1D structures with fractal atomic surfaces

A 1D structure with a *fractal atomic surface* (Hausdorff dimension 0.9157...) can be derived from the Fibonacci sequence by squaring its substitution matrix S:

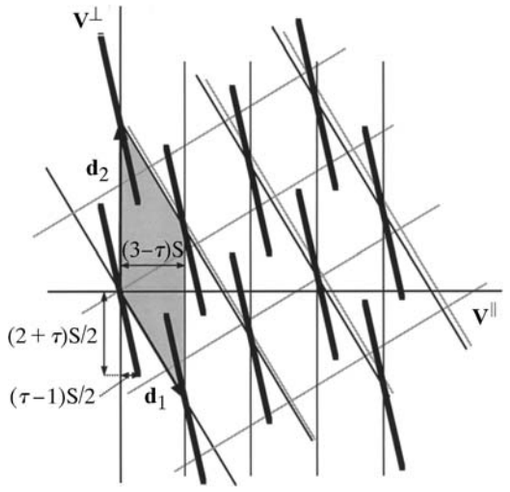

Fig. 4.6.2.11. 2D direct-space embedding of the Fibonacci chain as a modulated structure. The average period is $(3-\tau)$S. The square lattice in the quasicrystal description shown in Fig. 4.6.2.8 is indicated by grey lines. The rod-like atomic surfaces are now inclined relative to $\mathbf{V}^{\parallel}$ and arranged so as to give a saw-tooth modulation wave.

$$\begin{pmatrix} \mathrm{S} \\ \mathrm{L} \end{pmatrix} \rightarrow \begin{pmatrix} 1 & 1 \\ 1 & 2 \end{pmatrix} \begin{pmatrix} \mathrm{S} \\ \mathrm{L} \end{pmatrix} = \begin{pmatrix} \mathrm{S}+\mathrm{L} \\ \mathrm{S}+2\mathrm{L} \end{pmatrix}$$
$$\text{with } S^2 = \begin{pmatrix} 1 & 1 \\ 1 & 2 \end{pmatrix},$$

corresponding to the substitution rule S $\rightarrow$ SL, L $\rightarrow$ LLS as well as two other non-equivalent ones (see Janssen, 1995). The eigenvalues λ_i are obtained by calculating

$$\det |S - \lambda I| = 0.$$

The evaluation of the determinant gives the characteristic polynomial

$$\lambda^2 - 3\lambda + 1 = 0,$$

with the solutions $\lambda_{1,2} = [3 \pm (5)^{1/2}]/2$, with $\lambda_1 = \tau^2$ and $\lambda_2 = 1/\tau^2 = 2 - \tau$, and the same eigenvectors

$$\mathbf{w}_1 = \begin{pmatrix} 1 \\ \tau \end{pmatrix}, \quad \mathbf{w}_2 = \begin{pmatrix} 1 \\ -1/\tau \end{pmatrix}$$

as for the Fibonacci sequence. Rewriting the eigenvalue equation gives

$$\begin{pmatrix} 1 & 1 \\ 1 & 2 \end{pmatrix} \begin{pmatrix} 1 \\ \tau \end{pmatrix} = \begin{pmatrix} \tau+1 \\ 2\tau+1 \end{pmatrix} = \begin{pmatrix} \tau^2 \\ \tau^3 \end{pmatrix} = \tau^2 \begin{pmatrix} 1 \\ \tau \end{pmatrix}.$$

Identifying the eigenvector

$$\begin{pmatrix} 1 \\ \tau \end{pmatrix}$$

with

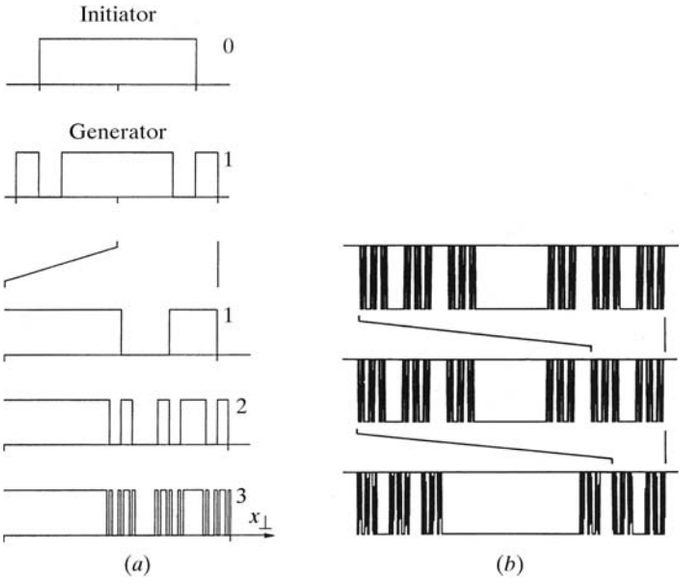

Fig. 4.6.2.12. (*a*) Three steps in the development of the fractal atomic surface of the squared Fibonacci sequence starting from an initiator and a generator. The action of the generator is to cut a piece from each side of the initiator and to add it where the initiator originally ended. This is repeated, cutting thinner and thinner pieces each time from the generated structures. (*b*) Magnification sequence of the fractal atomic surface illustrating its self-similarity. Each successive figure represents a magnification of a selected portion of the previous figure (from Zobetz, 1993).

$$\begin{pmatrix} \mathrm{S} \\ \mathrm{L} \end{pmatrix}$$

shows that the infinite 1D sequence $s(\mathbf{r})$ multiplied by powers of its eigenvalue τ^2 (scaling operation) remains invariant (each new lattice point coincides with one of the original lattice):

$$s(\tau^2\mathbf{r}) = s(\mathbf{r}).$$

The fractal sequence can be described on the same reciprocal and direct bases as the Fibonacci sequence. The only difference in the 2D direct-space description is the fractal character of the perpendicular-space component of the hyperatoms (Fig. 4.6.2.12) (see Zobetz, 1993).

4.6.3. Reciprocal-space images

4.6.3.1. Incommensurately modulated structures (IMSs)

One-dimensionally modulated structures are the simplest representatives of IMSs. The vast majority of the one hundred or so IMSs known so far belong to this class (Cummins, 1990). However, there is also an increasing number of IMSs with 2D or 3D modulation. The dimension d of the modulation is defined by the number of rationally independent modulation wavevectors (satellite vectors) $\mathbf{q}_i$ (Fig. 4.6.3.1). The electron-density function of a dD modulated 3D crystal can be represented by the Fourier series

$$\rho(\mathbf{r}) = (1/V)\sum_{\mathbf{H}} F(\mathbf{H}) \exp(-2\pi i \mathbf{H} \cdot \mathbf{r}).$$

The Fourier coefficients (*structure factors*) $F(\mathbf{H})$ differ from zero only for reciprocal-space vectors $\mathbf{H} = \sum_{i=1}^{3} h_i \mathbf{a}_i^* + \sum_{j=1}^{d} m_j \mathbf{q}_j = \sum_{i=1}^{3+d} h_i \mathbf{a}_i^*$ with $h_i, m_j \in \mathbb{Z}$. The d satellite vectors are given by $\mathbf{q}_j = \mathbf{a}_{3+j}^* = \sum_{i=1}^{3} \alpha_{ij} \mathbf{a}_i^*$, with α_{ij} a $3 \times d$ matrix σ. In the case of an